Band offset between cubic GaN and AlN from intra- and interband spectroscopy of superlattices

C. Mietze[1], E.A. DeCuir, Jr.[2], M.O. Manasreh[2], K. Lischka[1] and D.J. As[1]

[1]*University of Paderborn, Faculty of Science, Department of Physics, Warburger Strasse 100 D-33098 Paderborn, Germany*
[2]*Department of Electrical Engineering, University of Arkansas, 3217 Bell Engineering Center, Fayetteville, Arkansas 72701, USA*

Abstract. By the analysis of intra- and intersubband transitions in GaN/AlN superlattices the band offset is determined experimentally. Superlattice structures with different period lengths were fabricated by plasma-assisted molecular beam epitaxy 3C-SiC substrates. The structural properties were studied by high resolution X-ray diffraction, revealing a high structural perfection of the superlattice region with several peaks in the X-ray spectra. Infrared absorbance spectroscopy revealed clear intrasubband transitions in the spectral region of 1.55 μm measured at room temperature. Clear intersubband transitions were observed by photoluminescence at room temperature. These transition energies were compared to calculated energies using a 1D Poisson Schrödinger solver. For the calculations standard parameters for cubic GaN and AlN were used, while the band offset between GaN and AlN was varied. Optimal agreement between experimental and theoretical data was obtained for a band offset $\Delta E_C : \Delta E_V$ of 55:45.

Keywords: cubic AlN and GaN, MBE, inter- and intrasubband transitions
PACS: 81.15 Hi, 68.65. Cd, 78.40 Fy

1. INTRODUCTION

Wide band gap materials, especially III-nitrides are materials of high interest for optoelectronic devices or high power devices. Due to the relatively large difference in the band gap energies between GaN and AlN these materials offer the possibility of fabricating devices with intrasubband transitions tunable over a large infrared spectral range [1]. In III-nitrides with wurtzite crystal structure strong internal piezoelectric fields are present at the heterointerfaces between GaN and AlN. These fields reduce transition probabilities for optical transitions e.g. in multi quantum well structures due to the quantum confined Stark effect. Thus semipolar and nonpolar III-nitrides are of growing interest in the last years. Another possibility to avoid build-in fields is the growth of zincblende crystal structure where no internal fields appear because of the crystal symmetry. For better understanding and fabrication of devices the conduction and valence band discontinuities of these heterostructures are badly needed.

In this paper we report on the growth of c-GaN/c-AlN superlattice (SL) structures with constant c-AlN barrier width and varying quantum well width. Intra- and intersubband transition energies are determined from photoluminescence and absorbance measurements. We compare measured intra- and intersubband transition energies to calculated energies using a 1D Poisson-Schrödinger solver. Intrasubband transition energies in SLs depend mainly on the conduction band offset between well and barrier material while intersubband transition energies depend on conduction and valence band discontinuities. For given band gap energies and widths of SL structures the calculated transition energies can be brought into agreement with measured values by variation of the ratio $\Delta E_C : \Delta E_V$.

2. EXPERIMENTAL

Our structures were grown by plasma assisted molecular beam epitaxy (MBE) on 10 μm thick 3C-SiC on top of Si (001) (NovaSiC). We used a substrate temperature of 720 °C for all samples. First a 115 nm thick cubic GaN (c-GaN) buffer layer was deposited on the substrate. On the buffer layer a 20 period superlattice consisting of c-GaN/c-AlN was grown. The SL was capped by another 115 nm c-GaN layer. Growth was controlled by reflection

169

high energy electron diffraction (RHEED) [2]. While the thickness of the c-GaN quantum wells (QWs) was varied (sample A 2.5 nm, sample B 1.8 nm, and sample C 1.6 nm) the thickness of the c-AlN barriers was 1.5 nm for sample A and B and 1.7 nm for sample C. The lattice parameter and the strain of our superlattices were determined using high resolution x-ray diffraction (HRXRD) ω-2θ scans and reciprocal space maps (RSM).

An intrasubband transition is a transition from the first conduction band miniband to the second conduction band miniband. Intrasubband transition energies were obtained from optical absorbance measurements using a Bruker Fouriertransform 125HR spectrometer consisting of a quartz-halogen source with a calcium fluoride beam splitter and a cooled InSb detector. The spectral range of this configuration reaches from 1 μm to 3 μm. Due to selection rules of intrasubband transitions incident light has to be coupled into the sample laterally. To increase absorption samples were cut into waveguides to enable multiple passages of incident light through the active region.

By photoluminescence spectroscopy (PL) intersubband transitions from the lowest conduction band subband to the highest valence band subband can be observed. For PL a He-Cd laser with an emission wavelength of 325 nm was used. The emitted light was detected using a Spex 270m monochromator in combination with a photomultiplier and a Hamamatsu C3866 photon counter. PL measurements were performed with the samples mounted in a liquid He bath cryostat which enabled measurements at temperatures of 2 K and 300 K.

A 1D Poisson-Schrödinger solver (1D Poisson) [3] is used to calculate the energy levels of the minibands. Besides QW and barrier thickness the band offset between c-GaN and c-AlN is varied to achieve optimal agreement between measured energy values from PL, absorbance and calculated values.

3. RESULTS AND DISCUSSION

3.1 High Resolution X-ray Diffraction

The strain and lattice parameter of the grown superlattice structures are investigated by HRXRD. Fig. 1 shows a RSM of the (113) reflex of sample A. Clearly two additional SL satellites are observed. From the position of the satellites one can infer that the SL is pseudomorphically strained on the c-GaN. Strain has to be taken into account for the calculation of the band structure because it modifies the band gap. Using a simulation tool based upon dynamical scattering theory (MadMax) [4, 5] one can also obtain the averaged thicknesses of the single layers of the superlattice, yielding the sample structures given in paragraph 2.
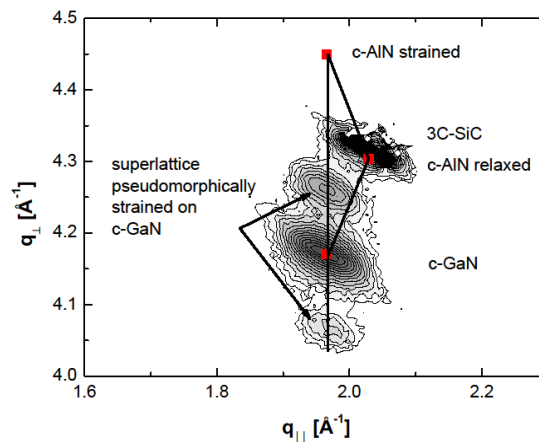

FIGURE 1 RSM of the (113) reflex of sample A. The positions of the two additional SL satellites reveal that the SL is pseudomorphically strained on the c-GaN buffer.

3.2 Intra- and Intersubband Transitions

The infrared absorbance spectra of our samples are plotted in Fig. 2a. The infrared absorbance (product of absorption coefficient α and QW thickness) is plotted versus the transition energy of the intrasubband transition. These spectra show clear evidence of intrasubband absorption due to the formation of minibands in the superlattice structure. The absorbance of sample B shows weak oscillations due to interference in the 10 μm thick 3C-SiC layer.

170

These oscillations are not observed in sample A and C most likely due to different interface roughnesses between 3C-SiC and Si.

Room temperature PL spectra of three different SL samples A, B and C are plotted in Fig. 2b. Besides the well known PL of bulk c-GaN [6] clear luminescence corresponding to the intersubband transition can be observed. All spectra were normalized to the SL peak intensity. The transition energy shifts to higher energies with descending well width.
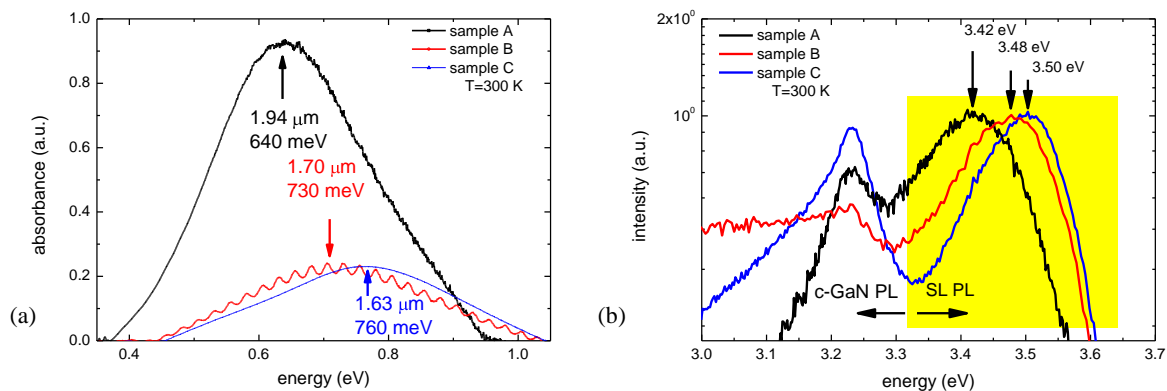
FIGURE 2 (a) Infrared absorbance spectra measured at room temperature. (b) Measured PL spectra at T=300 K. The yellow highlighted peaks can be related to intersubband transitions in the SL.

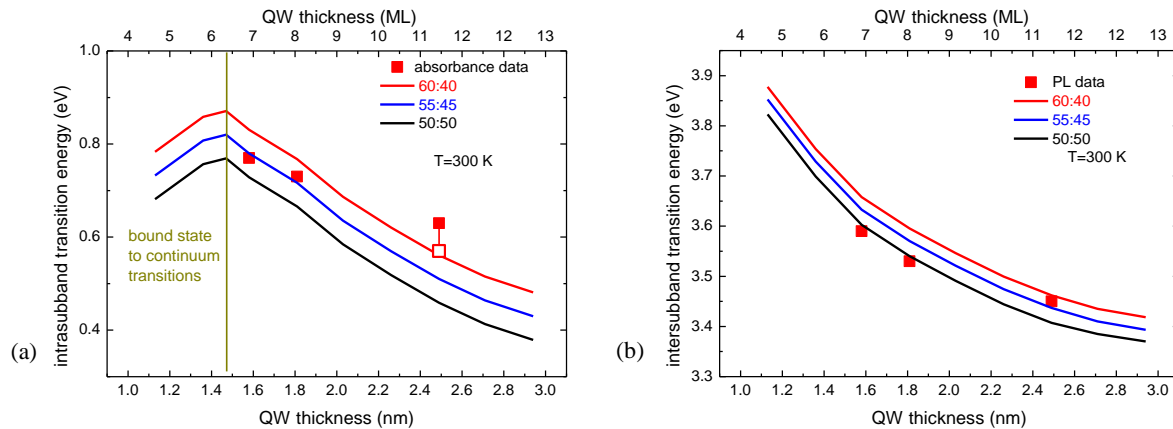## 3.3 Calculation of Transition Energies

The energy values of the bound states in our structures are calculated using 1D Poisson, a one dimensional Poisson-Schrödinger solver (1D Poisson) [6]. The transition energies are obtained from the differences of these calculated bound states.

As shown in the HRXRD RSM the c-AlN barriers are pseudomorphically strained on c-GaN. Due to the smaller lattice parameter of c-AlN compared to c-GaN c-AlN is tensile strained. Tensile strain reduces the band gap of a semiconductor which has to be taken into account for our calculations. Using Equation (1) a band gap for strained c-AlN of 5.69 eV is obtained [11] while the band gap of relaxed c-AlN is 5.9 eV [12]. The basic parameters of c-GaN and c-AlN used for the calculations can be found in [7-12].

$$E_{G,strained} = E_{G,0} + 2a_c\left(1 - \frac{c_{12}}{c_{11}}\right)\varepsilon_{xx} \tag{1}$$

As the energy height of an intrasubband transition for a fixed well- and barrier-width depends only on the conduction band offset between well and barrier material the transition energies are calculated for different conduction band offsets and therefore varying ratios of $\Delta E_C : \Delta E_V$ in order to find the values with the best agreement between calculation and experiment. For the three shown intrasubband transitions this ratio is varied between 30:70 and 70:30 with all other parameters fixed. Optimal fit between experiment and calculation is found for a conduction band discontinuity of (55 ± 5) % of the difference in band gap energies which is in the same order as published values for wurtzite GaN/AlN [13]. After the optimization of the parameters for intrasubband transitions these are used for calculation of intersubband transitions which also shows good agreement between calculated and measured values. Fig. 3a depicts a comparison between measured (red squares) and calculated (red, blue and black line) intrasubband transition energies for three different values of $\Delta E_C : \Delta E_V$. One can clearly observe that a ratio of 55:45 (blue line) represents the optimal parameter for this simulation. The calculated curves show a maximum for a well width of 1.45 nm which means that in thinner QWs the second bound state reaches the conduction band edge of the barrier and one can observe transitions from the first bound state to the continuum state. Using a barrier width of 1.5 nm for the sample with 2.5 nm QWs the transition energy would shift to a value as indicated in Fig.3a by the open square. Fig. 3b shows the measured PL results (red squares) in comparison to the calculated values (red, blue and black line) for the same band offset parameters. Due to the high exciton binding energy in c-GaN (larger than 25 meV) this energy has to be added to the measured values. It has also to be taken into account that this value shifts to even

171

higher energies in thin QWs which causes the deviation between experiment and calculation for the QWs with smaller width. Again optimal agreement between theory and experiment is found for a ratio of 55:45.

FIGURE 3 (a) Measured and calculated room temperature intrasubband transition energies versus QW thickness for different $\Delta E_C{:}\Delta E_V$ ratios. (b) Room temperature PL data in comparison to calculated transition energies for three different $\Delta E_C{:}\Delta E_V$ ratios.

4. CONCLUSION

Intra- and intersubband transition energies in c-GaN/c-AlN SL structures were obtained from measured photoluminescence and absorbance spectra. Intrasubband transitions in the spectral region from 2 μm - 1.6 μm could be observed using absorbance spectroscopy while the transition energies of the intersubband transition observed in PL varied between 3.3 eV and 3.65 eV. The presently unknown band offset between zincblende GaN and AlN was determined from intra- and intersubband transition energies of different SL structures. The ratio between conduction band and valence band discontinuity in c-GaN/c-AlN SLs was varied for optimal agreement between calculated and experimental data. We find a conduction band discontinuity of (55±5) % of the band gap differences for ΔE_C.

ACKNOWLEDGMENTS

REFERENCES

1. E.A. DeCuir, E. Fred, M.O. Manasreh, J. Schörmann, D.J. As, and K. Lischka, *Appl. Phys. Lett*. **91**, 041911 (2007).
2. J. Schörmann, S. Potthast, D.J. As, and K. Lischka, *Appl. Phys. Lett.* **90**, 041918 (2007).
3. I.H. Tan, G.L. Snider, L.D. Chang, and E.L. Hu, *J. Appl. Phys*. **68**, 4071 (1990).
4. O. Brandt, P. Waltereit, and K.H. Ploog, *Journal of Physics D: Appl. Physics*, **35,** 577-585 (2002).
5. O. Brandt, MadMax - Massively Accelerated Dynamical Multilayer Analysis by X-ray diffraction, Röntgen Simulationsprogramm, Copyright 1986, 1993, 1998 Thomas Williams, Colin Kelley.
6. D.J. As, F. Schmilgus, C. Wang, B. Schöttker, D. Schikora, and K. Lischka, *Appl. Phys. Lett*. **70**, 1311 (1997).
7. Y. Suzuki, M. Shinbara, H. Kii, and Y. Chikaura, *J. Appl. Phys*. **101**, 063516 (2007).
8. S. Pugh, D.J. Dugdale, S. Brand, and R.A. Abram, *Semicond. Sci. Techno.* **14**, 23 (1999).
9. C.G. van de Walle and J. Neugebauer, *Appl. Phys. Lett*. **70** (19), 2577 (1997).
10. K. Kim, W.R.L. Lambrecht, and B. Segall, Phys. Rev. B **53**, 16310 (1996).
11. I. Petrov, E. Mojab, R.C. Powell, and J.E. Greene, *Appl. Phys. Lett.* **60**, 2491 (1992).
12. M. Röppischer, R. Goldhahn, G. Rossbach, P. Schley, C. Cobet, N. Esser, T. Schupp, K. Lischka, D.J. As, *J. Appl. Phys.* **106** (7), 076104 (2009).
13. A.N. Westmeyer, S.Mahajan, K.K. Bajaj, J.Y. Lin, H.X. Jiang, D.D. Koleske, and R.T. Senger, *J. Appl. Phys.* **99**, 013705 (2006)